THE JOURNAL OF PHYSICAL CHEMISTRY C

Article

pubs.acs.org/JPCC

Zeolite Structures Loading with an Anticancer Compound As Drug Delivery Systems

Ricardo Amorim,[†] Natália Vilaça,[‡] Olga Martinho,[†] Rui M. Reis,[†,§] Mariana Sardo,[#] João Rocha,[#] António M. Fonseca,[‡] Fátima Baltazar,*[,†] and Isabel C. Neves*[,‡]

[‡]Center of Chemistry, Chemistry Department, University of Minho, Campus de Gualtar, 4710-057 Braga, Portugal

[†]Life and Health Sciences Research Institute (ICVS), School of Health Sciences/ICVS/3B's – PT Government Associate Laboratory, University of Minho, Campus de Gualtar, 4710-057 Braga/Guimarães, Portugal

[§]Molecular Oncology Research Center, Barretos Cancer Hospital, Barretos, São Paulo, Brazil

[#]CICECO – Chemistry Department, University of Aveiro, Campus de Santiago, 3810-193 Aveiro, Portugal

ABSTRACT: Two different structures of zeolites, faujasite (FAU) and Linde type A (LTA), were studied to investigate their suitability for drug delivery systems (DDS). The zeolites in the sodium form (NaY and NaA) were used as hosts for encapsulation of α-cyano-4-hydroxycinnamic acid (CHC). CHC, an experimental anticancer drug, was encapsulated in both zeolites by diffusion in liquid phase. These new drug delivery systems, CHC@zeolite, were characterized by spectroscopic techniques (FTIR, ^{1}H NMR, ^{13}C and ^{27}Al solid-state MAS NMR, and UV–vis), chemical analysis, powder X-ray diffraction (XRD) and scanning electron microscopy (SEM). The effect of the zeolites and CHC@zeolite drug deliveries on HCT-15 human colon carcinoma cell line viability was evaluated. Both zeolites alone revealed no toxicity to HCT-15 cancer cells. Importantly, CHC@zeolite exhibit an inhibition of cell viability up to 585-fold, when compared to the non-encapsulated drug. These results indicate the potential of the zeolites for drug loading and delivery into cancer cells to induce cell death.

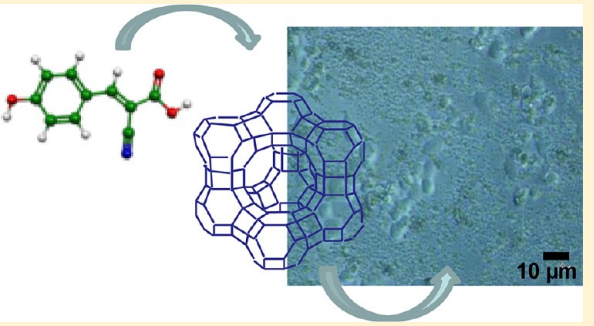

INTRODUCTION

Several inorganic materials are being explored as drug carriers opening new possibilities for biomedical applications.[1] Due to their biological properties and stability in biological environments, zeolites have been recently considered for medical use.[2,3] Zeolites are solid inorganic crystalline materials comprised of silicon, aluminum, and oxygen in the three-dimensional structure and the building blocks become arranged in a periodic way to form channels and cages on a nano- and subnanometer scale of strictly regular dimensions, named micropores.[4]

There are numerous examples of biomedical applications of zeolites reported in the literature including the enrichment and identification of low abundance peptides/proteins,[5] the immobilization of enzymes for biosensing,[6] for processes in magnetic resonance imaging,[6−10] in wound treatment,[11] and as drug delivery systems (DDS).[12−16] In DDS, the zeolitic structures and drugs could be simultaneously administrated to a patient without loss of the individual pharmacological effect of each product.[17−20] However, relatively fewer studies have been reported exploring the potential of zeolites as DDS for cancer applications. The latest experimental studies, based on the results obtained in various tumor cells and in tumor bearing animals, have shown that zeolites can be successfully applied as adjuvants in anticancer therapy.[21] In this context, we have previously reported the preparation of a DDS based in zeolite Y with an anticancer drug and demonstrated its efficacy against colorectal carcinoma (CRC) cells in vitro.[22] CRC is the most common type of tumor in Western countries, being men slightly more often affected.[23] Treatment of CRC includes surgery, radiotherapy, and/or chemotherapy. However, the treatment design depends largely on the cancer stage. Despite the progress made with the introduction of new cytotoxic agents[24−28] and medical practices, survival rates of patients with CRC changed little over the last 20 years,[29] justifying the need for more effective therapies and new drugs.

α-Cyano-4-hydroxycinnamic acid (CHC) is a compound derived from cinnamic acid and is a competitive inhibitor of monocarboxylate transporter 1 (MCT1),[30] a protein recently shown to be upregulated in colorectal and other cancers and thus a potential target for cancer therapy.[31−33] Published data demonstrated the cytotoxic and cytostatic effectiveness of CHC,[34,35] both in vitro and in vivo.[36,37] CHC used here in a model of colon carcinoma was chosen as a guest in two different structures of zeolites for drug delivery. Due to their structural properties, zeolites have attracted much research

Received: September 21, 2012
Revised: November 7, 2012

 © XXXX American Chemical Society dx.doi.org/10.1021/jp3093868 | J. Phys. Chem. C XXXX, XXX, XXX–XXX

attention for their potential application in the fields of biotechnology, selective adsorption, heterogeneous catalysis, polymer catalytic degradation, and functional materials.[4,38−41]

The faujasite framework of zeolite Y is based on sodalite cages that are joined by oxygen bridges between the hexagonal faces. Eight sodalite cages are linked together, forming a large central cavity or supercage with a diameter of 1.18 nm. The supercages share a 12-membered ring with an open diameter of 0.74 nm.[42] However, zeolite A exhibits LTA (Linde Type A) structure with small pores. The pore diameter is defined by an eight-member oxygen ring with an open diameter of 0.42 nm. This leads into a larger cavity of minimum free diameter 1.14 nm. The cavity is surrounded by eight sodalite cages (truncated octahedra), connected by their square faces in a cubic structure.[43−45]

In this study, we present the results obtained with two different synthetic structures of zeolites, faujasite (FAU) and Linde type A (LTA), and their suitability as drug delivery systems (DDS) for the anticancer drug CHC. The zeolites in sodium form (NaY and NaA) were used for encapsulation of CHC as a guest by diffusion in the liquid phase in the void space of the host zeolite porosity. The effect of the CHC concentration in both zeolites was studied. These new DDS were characterized by different methods (FTIR, ^{1}H NMR, ^{13}C and ^{27}Al solid-state MAS NMR, UV−vis, SEM, XRD, and elemental analysis). The effect of the zeolites and CHC@zeolite DDS was evaluated on HCT-15 human colon carcinoma cell viability.

EXPERIMENTAL SECTION

Preparation and Characterization of DDS. The zeolitic structures are commercially available; FAU zeolite in powder form (CBV100) was obtained from Zeolyst International and Linde type A zeolite from Sigma-Aldrich (European Commission, Institute for Reference Materials and Measurements, BCR-705). Zeolite NaA was available in pellet form with clay impurities and was transformed in powder before use. The encapsulation of CHC (α-cyano-4-hydroxycinnamic acid, Sigma-Aldrich) in zeolites was based on a previously established procedure.[20] Zeolites were dehydrated at 120 °C overnight, prior to insertion of the drug, to avoid the presence of water inside the pores, which renders the adsorption of the drug molecules more difficult. CHC encapsulation into the zeolites was achieved as follows: 500 mg of each zeolite with different Si/Al atomic ratios, NaY (Si/Al ratio = 2.83) and NaA (Si/Al ratio = 1.24) was reacted with a solution of 49.20 mg of CHC (0.26 mmol) in acetone (15 mL, Merck analytical grade), as a solvent. This mixture was carried out by stirring at room temperature for 48 h. During this time, the original white color of zeolites changed to the characteristic color of the CHC, yellow, indicating that the drug species were effectively incorporated inside the host. This finding was also confirmed by the disappearance of the yellow color of the starting CHC solution after 3 h in contact with the zeolite and the efficiency of the encapsulation was screened by HPLC.

The mixture was filtered and the yellow solid was dried in an oven at 60 °C for 12 h. This temperature is enough to evaporate the acetone solvent. Two other samples with different CHC concentrations, 98.40 mg of CHC (0.52 mmol) and 246.00 mg of CHC (1.30 mmol), were prepared in both zeolites under the same experimental conditions. The obtained DDS were denoted as CHC@zeolite$_n$, where n represents the CHC:zeolite ratio. The drug loading in the zeolites was determined by gravimetric analysis. In this technique, loading was obtained between the difference in weights of the powder starting zeolite and the DDS prepared by using an analytical balance (Precisa 40SM-200A ± 0.00001 g). In order to evaluate the solvent effect, the zeolites were prepared with 15 mL of solvent, using the same experimental conditions as the CHC@zeolites samples.

Characterization Methods. ^{13}C cross-polarization/magic angle spinning nuclear magnetic resonance (^{13}C CP/MAS NMR) and MAS ^{27}Al spectra were recorded on a 9.4 T wide-bore (400 MHz, ^{1}H Larmor frequency) Bruker Avance spectrometer. A 4 mm double-resonance MAS probe was employed at 100.6 (^{13}C) and 104.2 MHz (^{27}Al) Larmor frequencies. Samples were spun in ZrO_2 rotors, using a spinning rate of 14 kHz. ^{13}C CP/MAS NMR spectra were recorded with use of a ramp step (varying from 100% to 50% in amplitude using 100 points); contact time: 3.0 ms; ^{1}H 90° excitation pulse: 2.5 μs; ^{1}H and ^{13}C radio frequency field strengths for CP were set to 87 and 68 kHz, respectively; recycle delay: 5 s. TPPM-15 decoupling was employed during the signal acquisition, using a 4.75 μs pulse length for the basic TPPM pulse unit along the ^{1}H channel, employing a ^{1}H radio frequency field strength of 100 kHz. For the ^{27}Al MAS experiments, a 0.50 μs pulse length was applied, equivalent to a flip angle of 10°. ^{13}C chemical shifts are quoted in parts per million (ppm) from TMS and calibrated with respect to the external reference, glycine (CO, 176.03 ppm). All ^{27}Al chemical shifts were referenced with respect to an aqueous solution of $Al(NO_3)_3$. All samples were kept in a sealed container and exposed to a saturated solution of K_2SO_4 (relative humidity of 97%) for two weeks, prior to the acquisition of solid-state NMR data. This experimental protocol was necessary to guarantee the full hydration of the samples and therefore the reproducibility of the results. The quantitative analysis (Si, Al, and Na) was carried out by Inductively Coupled Plasma Atomic Emission Spectrometry (ICP-AES), using a Philips ICP PU 7000 spectrometer. Elemental analyses for carbon, nitrogen, and hydrogen were carried out on LECO CHNS-932 equipment. Samples were combusted at 1000 °C for 3 min with helium used as the purge gas. ^{1}H NMR spectra were obtained on a Varian Unity Plus spectrometer at an operating frequency of 300 MHz, using the solvent peak as internal reference at 25 °C, chemical shifts of protons being given in ppm using δ_H Me_4Si = 0 ppm as reference. The electronic UV−visible absorption spectra of drug and residual solutions were collected in the range 600−200 nm in a Shimadzu UV/2501PC spectrophotometer, using quartz cells at room temperature. Phase analysis was performed by XRD with a Philips PW1710 diffractometer. Scans were taken at room temperature in a 2θ range between 5° and 60°, using Cu Kα radiation. Scanning electron micrographs (SEM) were collected on a LEICA Cambridge S360 scanning microscope equipped with an EDX system. To avoid surface charging, samples were coated with gold under vacuum prior to analysis, using a Fisons Instruments SC502 sputter coater. The analysis was carried out by high performance liquid chromatography (HPLC JASCO 980-PU), using an isocratic pump and a double on line detection including an UV−vis detector and refractometer. Room temperature Fourier transform infrared (FTIR) spectra of the samples in KBr pellets (2 mg of sample was mixed in a mortar with 200 mg of KBr) were measured with a Bomem MB104 spectrometer in the range 4000−500 cm^{-1} by averaging 20 scans at a maximum resolution of 4 cm^{-1}.

dx.doi.org/10.1021/jp3093868 | J. Phys. Chem. C XXXX, XXX, XXX−XXX

Cell Culture Conditions. Human colon carcinoma-derived cell line HCT-15 was kindly provided by Dr. Raquel Seruca, (IPATIMUP, Porto, Portugal). HCT-15 colon carcinoma cells were maintained in RPMI 1640 medium (Gibco), supplemented with 10% (v/v) fetal bovine serum (FBS) (Gibco, Invitrogen, USA) and 1% (v/v) penicillin-streptomycin solution (P/S) (Invitrogen, USA) and incubated at 37 °C in a 5% CO_2 humidified atmosphere. Cells were subcultured approximately every three days and maintained in a log-phase growth.

Cell Viability Assays. Cell viability was assessed using the *In Vitro* Toxicology Assay Kit, Sulforhodamine B based (Sigma-Aldrich, St. Louis, MO, USA). HCT-15 cells were seeded in 96-well plates (5000 cells/100 μL/well) and incubated at 37 °C in a 5% CO_2 humidified atmosphere for 24 h. To assess the effects of the starting zeolites and the CHC@zeolite systems used (NaA and NaY), cells were incubated with increasing concentrations of the systems in culture medium. Controls were performed with culture medium alone. After an incubation period of 24 h, the spent media were removed and the plate wells were washed with 1× Phosphate-buffered solution, pH 7.4 (PBS). After a fixation step with cold 10% trichloroacetic acid (TCA), cells were stained with 0.4% Sulforhodamine B and the incorporated dye was solubilized with Sulforhodamine B solubilization solution (10 mM Tris). Absorbance was monitored with a microplate reader at 570 nm with a background absorbance of 655 nm. Cell viability was determined as percentage of viability: (OD experiment/OD control) × 100 (%). Results are presented as mean ± standard deviation (SD) of three independent experiments, each in triplicate. One-way ANOVA, followed by Dunnett post test was used to perform cell viability assay statistical analysis. The previous test and 50% growth inhibition (IC50) were determined with Graphpad Prism 5 software. Values were considered statistically significant in all experiments when $p < 0.05$.

RESULTS AND DISCUSSION

Preparation and Characterization of DDS. In the present study, the anticancer drug CHC was chosen to test the use of zeolite structures as DDSs. The approach for the preparation of DDS was the adsorption of CHC as a guest in liquid phase within the framework of the zeolite as a host. This approach required that the drug diffused inward the space available of the zeolite framework and the starting zeolites were not cytotoxic to the HCT-15 cell line. In this cell line, preliminary studies with NaY, NaMOR, NaA, and ZSM5 were also carried out. NaY (Faujasite) and NaA structures (Linde type A) showed to be nontoxic to the cells.

Table 1. Loading of CHC in the DDS

DDS	CHC (mmol)[a]	CHC (mmol)[b]	yield (%)[c]
CHC@$A_{1:10}$	0.260	0.198	76.2
CHC@$A_{2:10}$	0.520	0.377	72.5
CHC@$A_{5:10}$	1.300	0.876	67.4
CHC@$Y_{1:10}$	0.259	0.226	87.3
CHC@$Y_{2:10}$	0.517	0.438	84.8
CHC@$Y_{5:10}$	1.310	1.081	82.5

[a]Initial CHC amount in the solution. [b]CHC loading in zeolite. [c]Encapsulation efficiency of CHC in zeolites.

Both zeolites have different pore diameters, large pores for NaY (7.4 Å) and small pores for NaA (4.2 Å), which can determine the access of CHC into the structures. However, for CHC the length between the OH group from the aryl ring and the COOH is approximately 10.6 Å in the planar and linear molecule, and the aryl ring is 5.9 Å, suggesting that this drug could have some difficulty in diffusing into the NaA zeolite structure. The loading of CHC into the zeolites was determined by gravimetric analysis. Table 1 shows the loading obtained for all prepared DDS.

The residual drug content in solution after evaporation of the solvent is very low. In the case of NaY zeolite, around 85% of the CHC initially present has been retained inside this zeolite. However, for NaA, only 67−76% of the CHC was incorporated into the structure.

To confirm the integrity of the molecular structure of CHC after preparation of DDS, ^{1}H NMR and UV−vis experiments were performed with the residual drug solid obtained after filtration and pure CHC. The ^{1}H NMR spectra of the samples were recorded at 300 MHz in $CDCl_3$. The chemical shifts of protons observed for residual drug are δ 13.3 (s, COOH), 10.6 (s, OH), 8.3 (s, CH═), and 7.8 and 6.7 (2ddd, 4H from the aryl group). These chemical shifts of protons are in the same position as observed for the CHC pure molecule.[46] In the UV−vis spectrum, the presence of residual drug was evidenced by the appearance of an intense band (λ_{max} = 334 nm) in the same position of CHC in acetone (λ_{max} = 337 nm).[46] These results show that the encapsulation process preserved the integrity of CHC.

Preservation of the zeolite structures of the DDS was monitored by powder X-ray diffraction (XRD). The powder XRD diffraction patterns of the zeolites and encapsulated CHC were recorded at 2θ values between 5° and 60°. The parent zeolite Y sample is pure, while LTA is contaminated with a small amount of an unidentified phase displaying a main resonance at 26.6° 2θ probably due to the presence of clay in the pellet form. All samples exhibited XRD patterns similar to the patterns of the parent zeolites. No variation was observed in the characteristic peaks of zeolites after encapsulation of CHC, indicating that the frameworks did not undergo any significant structural change during the CHC encapsulation process. The XRD pattern of DDS prepared with NaY presented over 85% of crystallinity, while for NaA the crystallinity was ca. 75%.

The morphology of the DDS obtained after the encapsulation was observed by SEM analysis. Figure 1 shows the parent zeolites and the DDS with lower concentration of CHC.

The SEM micrographs of parent zeolites and the DDS indicate that no changes occur in the morphology and structure upon encapsulation of the drug. In panels a and c of Figure 1, it is clear from the micrographs of NaY and CHC@$Y_{1:10}$ that the morphology of the zeolite does not change after encapsulation of the CHC. The SEM microphotographs of the parent NaY and the DDS are typical of a microporous crystalline aluminosilicate structure with regular small particles.[47,48] The average of the particle diameter of the starting NaY was about 0.4−1.0 μm and the DDS preserved the same diameter. The starting NaA (Figure 1b) and its DDS (Figure 1d), two types of particles with different dimensions, can be observed: (i) aggregates of particles with a diameter of ∼2.6−5.0 μm and (ii) particles with a diameter of ∼0.3−1.0 μm. However, for both DDS, the energy-dispersive X-ray analysis plots detected the presence of nitrogen from the CHC molecule on the spotted surface.

dx.doi.org/10.1021/jp3093868 | J. Phys. Chem. C XXXX, XXX, XXX−XXX

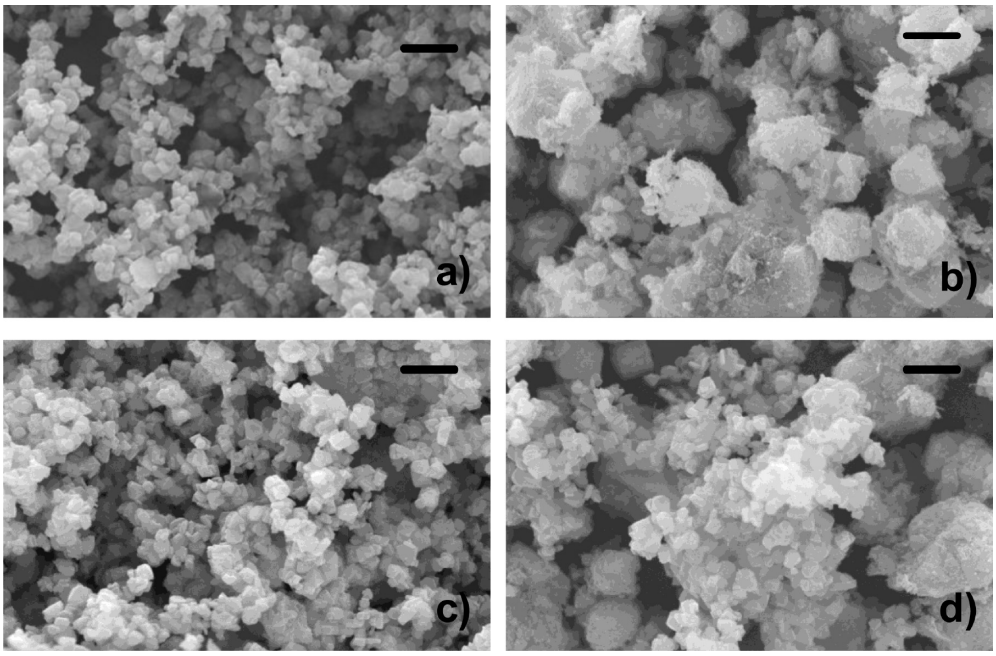

Figure 1. Scanning electron microscopy (SEM) images of zeolites and DDS herein studied. Scale bars represent 5 μm: NaY (a), NaA (b), CHC@$Y_{1:10}$ (c), and CHC@$A_{1:10}$ (d) with the same resolution (×5000).

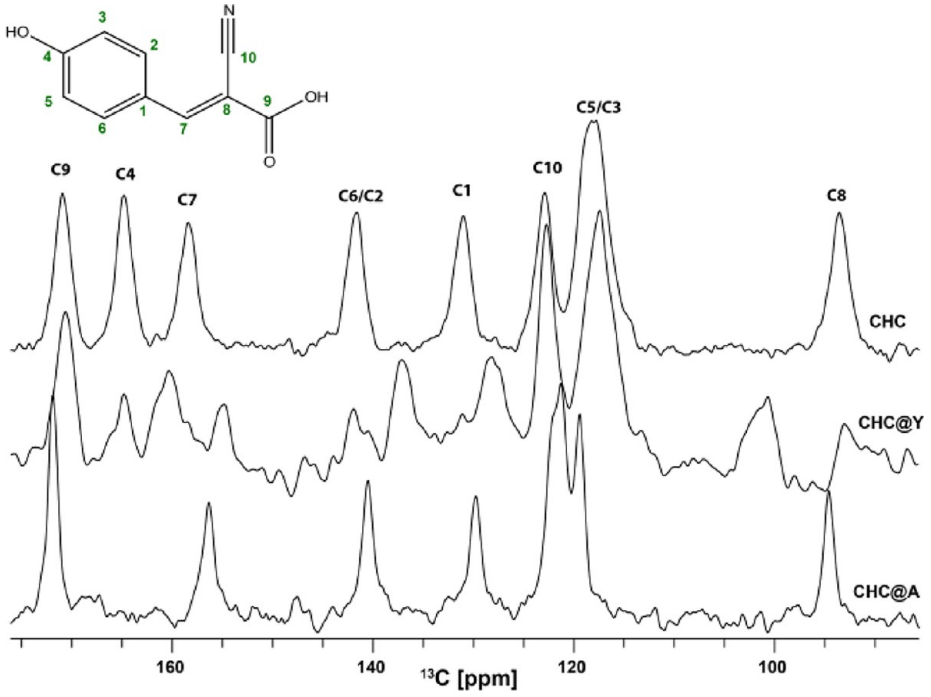

Figure 2. ^{13}C CP/MAS NMR spectra of CHC, CHC@$Y_{1:10}$, and CHC@$A_{1:10}$.

The integrity of the CHC in zeolites was confirmed by the analytical data of carbon and nitrogen content obtained by elemental analysis. The theoretical C/N ratio for CHC is 8.6 (63.49% to C and 7.40% to N). All samples based in different zeolites present a similar C/N ratio. For example, the guest C/N ratio obtained for CHC@$Y_{1:10}$ is 8.7 (1.66% to C and 0.19% to N) and for CHC@$A_{1:10}$ it is 8.3 (1.49% to C and 0.18% to N), indicating the presence of the molecular drug structure in the zeolite.

Evidence for the interaction between CHC and the zeolites is forthcoming from spectroscopic data. The ^{13}C CP/MAS NMR spectra of CHC, CHC@$Y_{1:10}$, and CHC@$A_{1:10}$ are shown in Figure 2.

The spectrum of CHC shows the characteristic peaks of the drug molecule, consistent with the assignment previously reported for similar compounds.[49] Peaks in the same spectral regions appear in both encapsulated zeolites, indicating the presence of CHC in the pores of the materials. The differences between the spectra of the pure and the zeolite-encapsulated samples are attributed to drug interactions with and/or conformational changes induced by the presence of Na^+ ions,

dx.doi.org/10.1021/jp3093868 | J. Phys. Chem. C XXXX, XXX, XXX−XXX

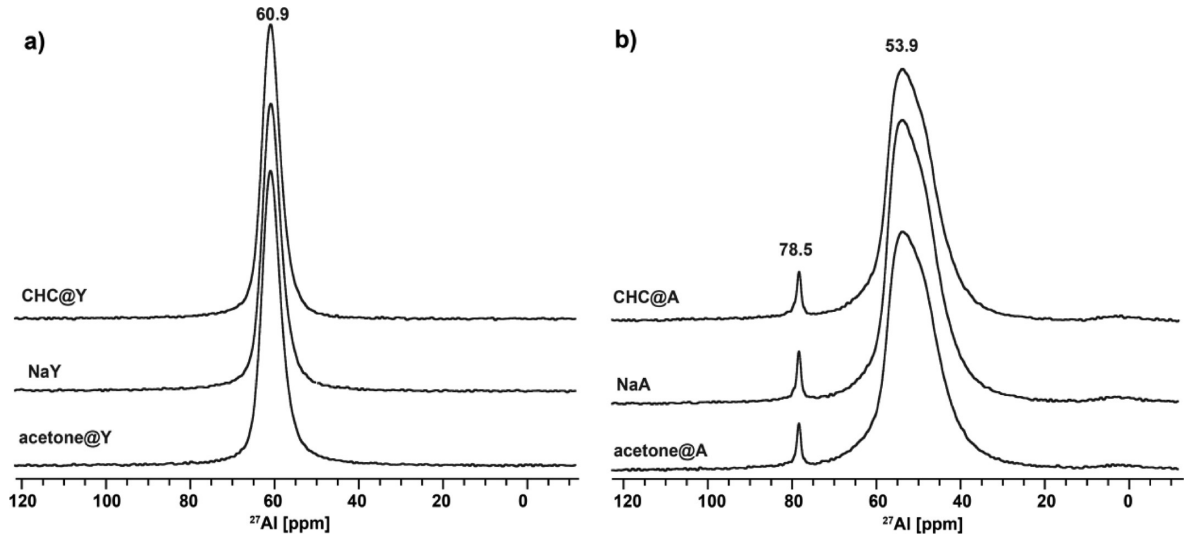

Figure 3. ^{27}Al MAS NMR spectra of parent Y (a) and LTA (b) zeolites and in the presence of solvents: acetone@zeolite and CHC@zeolite$_{1:10}$.

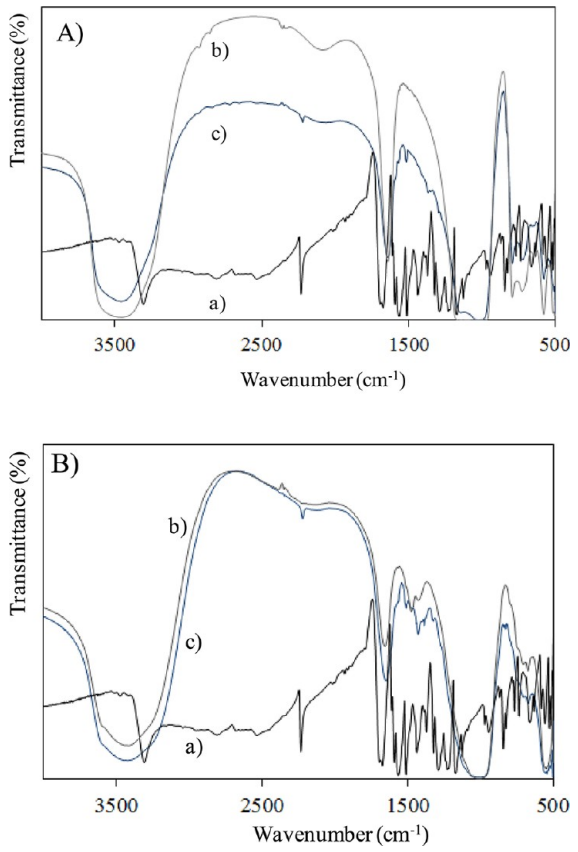

Figure 4. FTIR spectra of NaY (A) and NaA (B) for CHC (a), zeolites (b), and CHC@zeolite$_{1:10}$ (c).

Table 2. Final Assay Concentrations of CHC in the Different DDS

	DDS 1.00 mg/mL (mM)	DDS 0.25 mg/mL (mM)	DDS 0.10 mg/mL (mM)	DDS 0.05 mg/mL (mM)
CHC@A$_{1:10}$	0.198	0.050	0.020	0.010
CHC@A$_{2:10}$	0.377	0.094	0.038	0.019
CHC@A$_{5:10}$	0.876	0.219	0.088	0.044
CHC@Y$_{1:10}$	0.226	0.057	0.023	0.011
CHC@Y$_{2:10}$	0.435	0.109	0.044	0.022
CHC@Y$_{5:10}$	1.081	0.270	0.108	0.054

water molecules, and/or the zeolite framework. These observations are consistent with the FTIR results (see below).

The effect of the solvent on the preparation of the samples was also studied by ^{27}Al MAS NMR. The ^{27}Al MAS NMR spectra of the parent zeolites, CHC@zeolites$_{1:10}$ and acetone@zeolites, are shown in Figure 3.

All samples contain four-coordinated aluminum framework species [Al(OSi)$_4$], as revealed by the peaks at 60.9 ppm for Y and 53.9 ppm for LTA samples. No shift or broadening of the ^{27}Al peaks were observed upon introduction of the solvent or upon drug-molecule encapsulation, including no changes in the octahedral-coordinated region (even if a faint broad peak at ca. 5 ppm, presumably from the impurity, is observed for all LTA samples), indicating that the experimental procedures do not provoke damages in the structure in agreement with XRD and SEM analyses. The same behavior was observed in the ^{23}Na solid-state MAS NMR spectra. The faint and sharp ^{27}Al resonance at 78.5 observed in the spectra of the LTA samples (Figure 3b) is assigned to the unknown impurity contaminating the parent sample and also revealed by XRD.

The presence of the drug and its interactions in both zeolites are also screened by Fourier transformed infrared spectroscopy (FTIR). Figure 4 shows the infrared spectra of NaY (A) and NaA (B) for CHC (a), zeolites (b), and CHC@zeolite$_{1:10}$ (c).

The FTIR spectrum of CHC (Figure 4a) shows the presence of ν(C≡N) at 2230 cm^{-1}, ν(C═O) at 1678 cm^{-1}, and the vibrational bands characteristic of the C—C and C—H groups around 1550 and 1150 cm^{-1}. For the prepared DDS, the FTIR spectra of zeolites and the samples are dominated by the strong bands assigned to the vibration of the zeolite structure. The presence of physisorbed water is detected by the ν(O—H) stretching vibration at 3410 cm^{-1} and the ν(O—H) deformation band at 1635 cm^{-1}. The bands corresponding to the lattice vibrations are observed in the spectral region between 1300 and 450 cm^{-1}.[47,48]

dx.doi.org/10.1021/jp3093868 | J. Phys. Chem. C XXXX, XXX, XXX−XXX

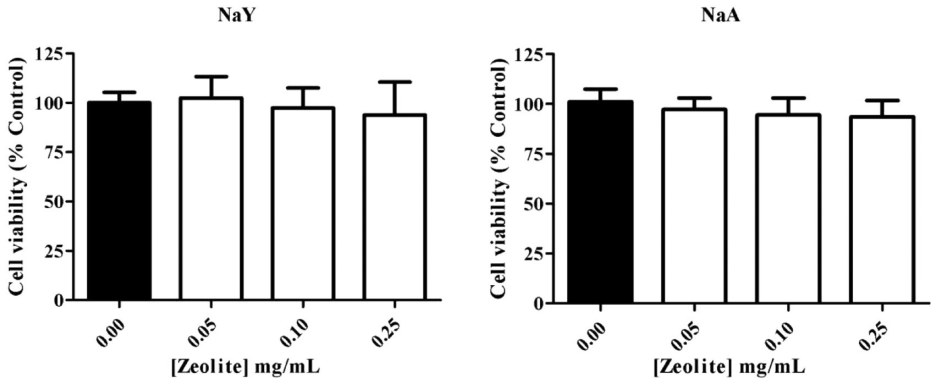

Figure 5. Effect of NaY and NaA zeolites on HCT-15 colon carcinoma cell viability. The HCT-15 cell line was incubated with the different zeolite concentrations for 24 h. Cell viability was measured by SRB assay. Values are means ± SD of three independent experiments, each performed in triplicate. $p < 0.05$, compared to the control bar (cells without zeolite).

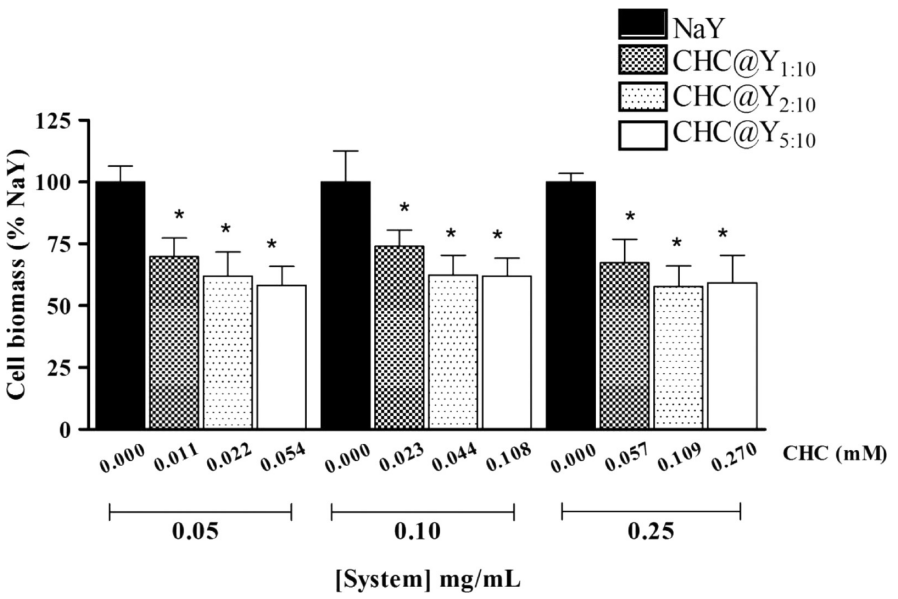

Figure 6. Effect of NaY zeolite and CHC@NaY systems on HCT-15 colon carcinoma cell viability. The HCT-15 cell line was incubated with NaY and different DDS concentrations for 24 h. Cell viability was measured by SRB assay. Values are means ± SD of three independent experiments, each performed in triplicate. The asterisk indicates $p < 0.05$, compared to the control bar (NaY).

In addition to these strong bands caused by the host zeolite, the FTIR spectra for CHC@zeolite$_{1:10}$ (Figure 4c) exhibits bands in the regions 2500−2000 cm^{-1} and 1600−1200 cm^{-1} where the zeolites do not absorb and they are attributed to the presence of the encapsulated drug. The spectra of the encapsulated as well as pure CHC showed similar bands. For example, the spectrum of CHC@A$_{1:10}$ shows bands from CHC at 2216, 1506, 1419, and 1311 cm^{-1}. No shift or broadening in the principal zeolite vibrational bands occur upon inclusion of the drug, further substantiating that the zeolite framework remains unchanged. Although the characteristic CHC FTIR vibrational bands in the CHC@zeolite spectra are weak, they provide evidence for the presence of drug in the zeolite. Due to overlap with the strong bands arising from the zeolite framework, it is not possible to draw any further conclusions from these data. NMR spectroscopy is, thus, much more sensitive to molecule structural changes than is FTIR.

Drug Bioactivity Studies. Working DDS concentrations (0.05, 0.10, and 0.25 mg/mL) were obtained by diluting a stock suspension (1.00 mg/mL) in culture medium (RPMI1640). For better homogenization, all suspensions were submitted to ultrasonic dispersion for 2 min prior to use. The concentrations of zeolite suspensions used in this work and the corresponding CHC final assay concentrations are presented in Table 2. t2

To be considered as suitable DDS, zeolites themselves should present small or no effect on cell viability. The cytotoxicity of the starting zeolites was investigated in the HCT-15 cell line. Figure 5 shows the effect of increasing f5 amounts of both zeolites NaY and NaA on the viability of HCT-15 cells, determined by the SRB assay.

The two zeolites used gave similar results. The differences between controls (without zeolite) and the range of zeolite concentrations are insignificant, showing in this way that both zeolites are nontoxic to the cells for the selected period of incubation. To verify whether the encapsulation of CHC into zeolites potentiates the effect of this monocarboxylate transporter (MCT) inhibitor, the effect of zeolite NaA and NaY loaded with different amounts of CHC was tested in HCT-15 cell viability with increasing concentrations of the CHC@ zeolite systems (0.05−0.25 mg/mL). Compared to NaY alone (control), there is an evident reduction in cell viability, from

dx.doi.org/10.1021/jp3093868 | J. Phys. Chem. C XXXX, XXX, XXX−XXX

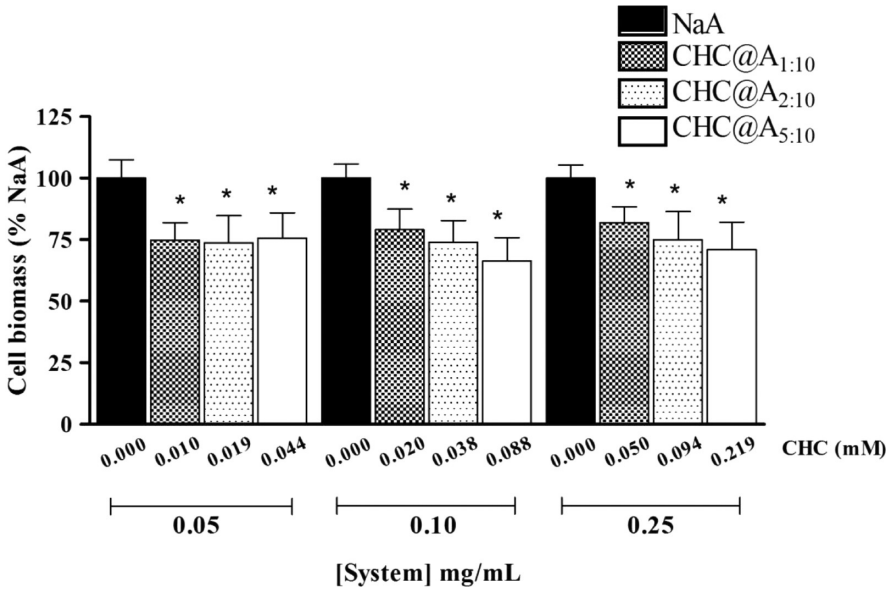

Figure 7. Effect of NaA zeolite and CHC@NaA systems on HCT-15 colon carcinoma cell viability. The HCT-15 cell line was incubated with NaA and different DDS concentrations for 24 h. Cell viability was measured by SRB assay. Values are means ± SD of three independent experiments, each performed in triplicate. Teh asterisk indicates $p < 0.05$, compared to the control bar (NaA).

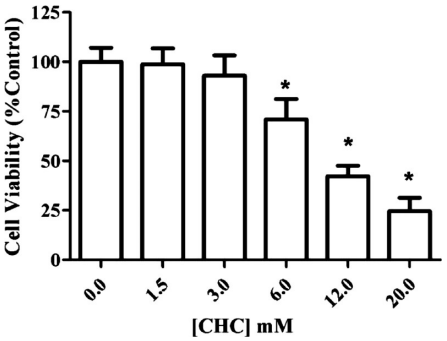

Figure 8. Effect of CHC on HCT-15 colon carcinoma cell viability. The HCT-15 cell line was incubated with increasing concentrations of CHC for 24 h. Cell viability was measured by SRB assay. Values are means ± SD of three independent experiments, each performed in triplicate. The asterisk indicates $p < 0.05$, compared to the control bar (vehicle, no CHC).

74% to 58%, with increasing concentrations of CHC in the zeolite system (Figure 6).

The cytotoxic effect of DDS with NaY was more pronounced for higher concentrations of CHC; however, the effect appears not to be directly proportional to the concentrations of the zeolite suspensions. For CHC@NaA, the cytotoxicity was not as high as for NaY zeolite, a reduction of cell viability from 82% to 66% was obtained when comparing with cells treated with the starting zeolite (Figure 7).

Figure 8 shows the effects on cell viability obtained when treating HCT-15 cells with the nonencapsulated CHC. Working concentrations (1.5, 3.0, 6.0, 12.0, and 20.0 mM) were obtained by diluting the stock solution (2.9 M) in culture medium (RPMI 1640). It is possible to observe a dose-dependent decrease in cell viability, being the IC_{30} and IC_{50} values of 6.43 mM and 10.26 mM, respectively.

By comparing the results obtained when treating the HCT-15 cells with the nonencapsulated CHC with the ones of encapsulated CHC, there is an obvious potentiation of the effect of the drug. A 6.43 mM concentration of the nonencapsulated drug is necessary for a 30% of inhibition of cell viability (IC_{30}) (Figure 8). In contrast, with the encapsulated drug, for the same magnitude of inhibition and for the 0.05 mg/mL of concentration zeolite suspension of the different system of CHC@Y, there is an increase in efficiency of the drug between 119- and 585-fold, corresponding to CHC assay concentrations of 0.054 and 0.011 mM, respectively (Table 2).

The studies for CHC@A showed a lower effect on in-cell viability when compared with NaY. For 30% inhibition of cell viability, using 0.05 mg/mL of concentration zeolite suspension of the CHC@A system, there is an efficiency of the drug effect between 29- and 146-fold, corresponding to CHC assay concentrations of 0.220 and 0.044 mM, respectively (Table 2).

NaY DDS was more effective than NaA DDS due to the more open structure of the zeolite Y, in which CHC could freely diffuse to the outside of the structure toward the cells. However, for higher concentrations of the system or parent zeolite (above 0.25 mg/mL), the cell viability begins to be affected, likely due to the compromise of cell-nutrient exchange with the culture media.

By encapsulating CHC into zeolites, we increased significantly the efficiency of this drug, which could be related to CHC solubility. Since it is a hydrophobic molecule, it is difficult to obtain a homogeneous solution with CHC. Thus, we believe that similarly to other systems,[50−53] the zeolite DDSs allow the slow release of CHC, increasing the bioavailability of the drug, and thus explaining this increase in potency. Another hypothesis, which would explain the high increase in potency, could be the promotion of CHC entry into the cell. It is described that CHC could inhibit the entry of pyruvate into the mitochondria, compromising the normal respiration of cells,[54] at much lower concentrations. Thus, this high potency could be the combined result of both the increase in CHC bioavailability and the promotion of CHC entry into the cell by the DDS.

dx.doi.org/10.1021/jp3093868 | J. Phys. Chem. C XXXX, XXX, XXX−XXX

CONCLUSIONS

The studies on the zeolites discussed here demonstrate that these structures can be used effectively for sustained release applications. Two different structures of zeolites, faujasite (FAU) and Linde type A (LTA), were prepared and characterized to assess their ability to encapsulate and release the experimental anticancer drug CHC. The effect of the zeolites and CHC@zeolite DDS on the HCT-15 human colon carcinoma cell line viability was evaluated. Both zeolites alone revealed no toxicity to HCT-15 cancer cells. Importantly, CHC@zeolite led to an inhibition of cell viability up to 585-fold when compared to the nonencapsulated drug. These results indicate the potential of the zeolites for drug loading and delivery to cancer cells.

AUTHOR INFORMATION

Corresponding Author

*E-mail: fbaltazar@ecsaude.uminho.pt (F.B.) and ineves@quimica.uminho.pt (I.C.N.).

Notes

The authors declare no competing financial interest.

ACKNOWLEDGMENTS

The authors are thankful to Dr. A. S. Azevedo for collecting the powder diffraction data. O.M. and R.A. are recipients of fellowships (SFRH/BD/36463/2007, SFRH/BI/51118/2010) from Fundação para a Ciência e a Tecnologia (FCT, Portugal). This work was supported by the FCT projects refs PEst-C/QUI/UI0686/2011, PEst-C/CTM/LA0011/2011, and PTDC/SAU-FCF/104347/2008, under the scope of "Programa Operacional Temático Factores de Competitividade" (COMPETE) of "Quadro Comunitário de Apoio III" and cofinanced by Fundo Comunitário Europeu FEDER, and the Centre of Chemistry and Life and Health Sciences Research Institute (University of Minho, Portugal).

REFERENCES

(1) Moyano, D. F.; Rotello, V. M. *Langmuir* **2011**, *27*, 10376−10385.
(2) Danilczuk, M.; Dugopolska, K.; Ruman, T.; Pogocki, D. *Mini-Rev. Med. Chem.* **2008**, *8*, 1407−1417.
(3) Fatouros, D. G.; Douroumis, D.; Nikolakis, V.; Ntais, S.; Moschovi, A. M.; Trivedi, V.; Khima, B.; Roldo, M.; Nazar, H.; Cox, P. A. *J. Mater. Chem.* **2011**, *21*, 7789−7794.
(4) Corma, A.; Garcia, H. *Eur. J. Inorg. Chem.* **2004**, *6*, 1143−1164.
(5) Zhang, Y. H.; Yu, X. J.; Wang, X. Y.; Shan, W.; Yang, P. Y.; Tang, Y. *Chem. Commun.* **2004**, 2882−2883.
(6) Corma, A.; Fornes, V.; Rey, F. *Adv. Mater.* **2002**, *14*, 71−74.
(7) Platas-Iglesias, C.; Van der Elst, L.; Zhou, W. Z.; Muller, R. N.; Geraldes, C. F. G. C.; Maschmeyer, T.; Peters, J. A. *Chem.—Eur. J.* **2002**, *8*, 5121−5131.
(8) Norek, M.; Neves, I. C.; Peters, J. A. *Inorg. Chem.* **2007**, *46*, 6190−6196.
(9) Tsotsalas, M. M.; Kopka, K.; Luppi, G.; Wagner, S.; Law, M. P.; Schafers, M.; De Cola, L. *ACS Nano* **2010**, *4*, 342−348.
(10) Ndiege, N.; Raidoo, R.; Schultz, M. K.; Larsen, S. *Langmuir* **2011**, *27*, 2904−2909.
(11) Galownia, J.; Martin, J.; Davis, M. E. *Microporous Mesoporous Mater.* **2006**, *92*, 61−63.
(12) Zhang, H.; Kim, Y.; Dutta, P. K. *Microporous Mesoporous Mater.* **2006**, *88*, 312−318.
(13) Arruebo, M.; Fernandez-Pacheco, R.; Irusta, S.; Arbiol, J.; Ibarra, M. R.; Santamaria, J. *Nanotechnology* **2006**, *17*, 4057−4064.
(14) Braschi, I.; Gatti, G.; Paul, G.; Gessa, C. E.; Cossi, M.; Marchese, L. *Langmuir* **2010**, *26*, 9524−9532.
(15) Braschi, I.; Blasioli, S.; Gigli, L.; Gessa, C. E.; Alberti, A.; Martucci, A. *J. Hazard. Mater.* **2010**, *178*, 218−225.
(16) Martucci, A.; Pasti, L.; Marchetti, N.; Cavazzini, A.; Dondi, F.; Alberti, A. *Microporous Mesoporous Mater.* **2012**, *148*, 174−183.
(17) Zarkovic, N.; Zarkovic, K.; Kralj, M.; Borovic, S.; Sabolovic, S.; Blazi, M. P.; Cipak, A.; Pavelic, K. *Anticancer Res.* **2003**, *23*, 1589−1595.
(18) Dyer, A.; Morgan, S.; Wells, P.; Williams, C. *J. Helminthol.* **2000**, *74*, 137−141.
(19) Farias, T.; Ruiz-Salvador, A. R.; Rivera, A. *Microporous Mesoporous Mater.* **2003**, *61*, 117−125.
(20) Rimoli, M. G.; Rabaioli, M. R.; Melisi, D.; Cucio, A.; Mondello, S.; Mirabelli, R.; Sbignete, E. *J. Biomed. Mater. Res., Part A* **2008**, *87A*, 156−164.
(21) Ceyhan, T.; Tatlier, M.; Akcakaya, H. *J. Mater. Sci. Mater. Med.* **2007**, *18*, 1557−1562.
(22) Vilaca, N.; Amorim, R.; Martinho, O.; Reis, R. M.; Baltazar, F.; Fonseca, A. F.; Neves, I. C. *J. Mater. Sci.* **2011**, *46*, 7511−7516.
(23) Jemal, A.; Siegel, R.; Ward, E.; Hao, Y.; Xu, J.; Murray, T.; Thun, M. J. *Ca-Cancer J. Clin.* **2008**, *58*, 71−96.
(24) Heidelberger, C.; Chaudhuri, N. K.; Danneberg, P.; Mooren, D.; Griesbach, L.; Duschinsky, R.; Schnitzer, R. J.; Pleven, E.; Scheiner, J. *Nature* **1957**, *179*, 663−666.
(25) Ciardiello, F.; Tortor, G. *Eur. J. Cancer* **2003**, *39*, 1348−1354.
(26) Kabbinavar, F.; Schulz, J.; McCleod, M.; Pattel, T.; Hamm, J.; Hecht, J. R.; Mass, R.; Perrou, B.; Nelson, B.; Novotny, W. F. *J. Clin. Oncol.* **2005**, *23*, 3697−3705.
(27) Giantonio, B. J. *Nat. Rev. Clin. Oncol.* **2009**, *6*, 311−312.
(28) Odom, D.; Barber, B.; Bennett, L.; Peeters, M.; Zhao, Z. Y.; Kaye, J.; Wolf, M.; Wiezorek, J. *Int. J. Colorectal Dis.* **2011**, *26* (2), 173−181.
(29) Ozols, R. F.; Herbst, R. S.; Colson, Y. L.; Gralow, J.; Bonner, J.; Curran, W. J.; Eisenberg, B. L.; Ganz, P. A.; Kramer, B. S.; Kris, M. G.; et al. *J. Clin. Oncol.* **2007**, *25*, 146−162.
(30) Halestrap, A. P.; Meredith, D. *Eur. J. Physiol.* **2004**, *447*, 619−628.
(31) Pinheiro, C.; Longatto-Filho, A.; Scapulatempo, C.; Ferreira, L.; Martins, S.; Pellerin, L.; Rodrigues, M.; Alves, V. A. F.; Schmitt, F.; Baltazar, F. *Virchows Archs.* **2008**, *452*, 139−146.
(32) Pinheiro, C.; Longatto-Filho, A.; Pereira, S. M. M.; Etlinger, D.; Moreira, M. A. R.; Jubé, L. F.; Queiroz, G. S.; Schmitt, F.; Baltazar, F. *Dis. Markers* **2009**, *26*, 97−103.
(33) Pinheiro, C.; Albergaria, A.; Paredes, J.; Sousa, B.; Dufloth, R.; Vieira, D.; Schmitt, F.; Baltazar, F. *Histopathology* **2010**, *56*, 860−867.
(34) Wahl, M. L.; Owen, J. A.; Burd, R.; Herlands, R. A.; Nogami, S. S.; Rodeck, U.; Berd, D.; Leeper, D. B.; Owen, C. S. *Mol. Cancer Ther.* **2002**, *1*, 617−628.
(35) Coss, R. A.; Storck, C. W.; Daskalakis, C.; Berd, D.; Wahl, M. L. *Mol. Cancer Ther.* **2003**, *2*, 383−388.
(36) Colen, C. B.; Seraji-Bozorgzad, N.; Marples, B.; Galloway, M. P.; Sloan, A. E.; Mathupala, S. P. *Neurosurgery* **2006**, *59*, 1313−1323.
(37) Sonveaux, P.; Végran, F.; Schroeder, T.; Wergin, M. C.; Verrax, J.; Rabbani, Z. N.; De Saedeleer, C. J.; Kennedy, K. M.; Diepart, C.; Jordan, B. F.; et al. *J. Clin. Invest.* **2008**, *118*, 3930−3942.
(38) Silva, B.; Figueiredo, H.; Soares, O. S. G. P.; Pereira, M. F. R.; Figueiredo, J. L.; Lewandowska, A. E.; Banares, M. A.; Neves, I. C.; Tavares, T. *Appl. Catal., B* **2012**, *117*, 406−413.
(39) Kuzniarska-Biernacka, I.; Biernacki, K.; Magalhães, A. L.; Fonseca, A. M.; Neves, I. C. *J. Catal.* **2011**, *278*, 102−110.
(40) Parpot, P.; Teixeira, C.; Almeida, A. M.; Ribeiro, C.; Neves, I. C.; Fonseca, A. M. *Microporous Mesoporous Mater.* **2009**, *117*, 297−303.
(41) Neves, I. C.; Botelho, G.; Machado, A. V.; Rebelo, P.; Ramôa, S.; Pereira, M. F. R.; Ramanathan, A.; Pescarmona, P. *Polym. Degrad. Stab.* **2007**, *92*, 1513−1519.
(42) Van Santen, R. A.; Kramer, G. J. *Chem. Rev.* **1995**, *95*, 637−660.
(43) Database of Zeolite Structures from the International Zeolite Association (IZA-SC): www.iza-structure.org/databases/.

588 (44) Baerlocher, Ch.; McCusker, L. B.; Olson, D. H. *Atlas of zeolite*
589 *framework types*; 6th revised ed.; Elsevier: Amsterdam, The Nether-
590 lands, 2007.
591 (45) Subhash, B. *Zeolite Catalysis: Principles and Applications*; CRC
592 Press, Inc.: Boca Raton, FL, 1990.
593 (46) Tarzi, O. I.; Nonami, H.; Erra-Balsells, R. *J. Mass Spectrom.*
594 **2009**, *44*, 260−277.
595 (47) Neves, I. C.; Cunha, C.; Pereira, M. R.; Pereira, M. F. R.;
596 Fonseca, A. M. *J. Phys. Chem. C* **2010**, *114* (24), 10719.
597 (48) Tanaka, K.; Choo, C.-K.; Komatsu, Y.; Hamaguchi, K.; Yamaki,
598 M.; Itoh, T.; Nishigaya, T.; Nakata, R.; Morimoto, K. *J. Phys. Chem. B*
599 **2004**, *108*, 2501−2508.
600 (49) Silva, A. M. S.; Alkorta, I.; Elguero, J.; Silva, V. L. M. *J. Mol.*
601 *Struct.* **2001**, *595*, 1−6.
602 (50) Gultepe, E.; Nagesha, D.; Sridhar, S.; Amiji, M. *Adv. Drug*
603 *Deliver Rev.* **2010**, *62*, 305−315.
604 (51) Anglin, E. J.; Cheng, L.; Freeman, Q. R.; Sailor, M. J. *Adv. Drug*
605 *Deliver Rev.* **2008**, *60*, 1266−1277.
606 (52) Vivero-Escoto, J. L.; Slowing, I. I.; Trewyn, B. G.; Lin, V. S.-Y.
607 *Small* **2010**, *6*, 1952−1967.
608 (53) Zhu, Y.; Ikoma, T.; Hanagata, N.; Kaskel, S. *Small* **2010**, *6*,
609 471−478.
610 (54) Halestrap, A. P.; Denton, R. M. *Biochem. J.* **1974**, *138*, 313−316.